

UWL REPOSITORY

repository.uwl.ac.uk

Time-resolved metabolic footprinting for nonlinear modeling of bacterial substrate utilization

Behrends, Volker, Ebbels, Tim MD, Williams, Huw D and Bundy, Jacob G (2009) Time-resolved metabolic footprinting for nonlinear modeling of bacterial substrate utilization. Applied and Environmental Microbiology, 75 (8). pp. 2453-2463. ISSN 0099-2240

http://dx.doi.org/10.1128/AEM.01742-08

This is the Accepted Version of the final output.

UWL repository link: https://repository.uwl.ac.uk/id/eprint/11448/

Alternative formats: If you require this document in an alternative format, please contact: <u>open.research@uwl.ac.uk</u>

Copyright: Creative Commons: Attribution 4.0

Copyright and moral rights for the publications made accessible in the public portal are retained by the authors and/or other copyright owners and it is a condition of accessing publications that users recognise and abide by the legal requirements associated with these rights.

Take down policy: If you believe that this document breaches copyright, please contact us at <u>open.research@uwl.ac.uk</u> providing details, and we will remove access to the work immediately and investigate your claim.

1	Time-resolved metabolic footprinting for non-linear modelling of				
2	bacterial substrate utilization				
3					
4	Volker Behrends ^{1,2} , Tim MD Ebbels ¹ , Huw D Williams ² , Jacob G Bundy ¹ *				
5					
6	1: Imperial College London, Department of Biomolecular Medicine, Division of				
7	Surgery, Oncology, Reproductive Biology, and Anaesthetics, Faculty of Medicine, Sir				
8	Alexander Fleming Building, London SW7 2AZ, UK				
9					
10	2: Imperial College London, Department of Life Sciences, Division of Biology, Faculty				
11	of Natural Sciences, Sir Alexander Fleming Building, London SW7 2AZ, UK				
12					
13	*Corresponding author.				
14	Email: j.bundy@imperial.ac.uk				
15	Telephone: +44 20 75943039				
16	Fax: +44 20 75943226				
17					
18	Running title: Time-resolved metabolic footprinting				
19					
20	Keywords: metabolomics, <i>Pseudomonas aeruginosa</i> , <i>Burkholderia cepacia</i> complex,				
21	Escherichia coli, metabolic footprinting, exometabolome, cystic fibrosis				
22					

1 ABSTRACT

Untargeted profiling of small molecule metabolites from microbial culture 2 supernatants (metabolic footprinting) has great potential as a phenotyping tool. We 3 4 employed time-resolved metabolic footprinting to compare one Escherichia coli and three *Pseudomonas aeruginosa* strains growing on complex media and showed that 5 considering metabolite changes over the whole course of growth provides much 6 more information than taking a single time-point. Most strikingly, there was 7 8 pronounced selectivity in metabolite uptake, even when the bacteria were growing apparently exponentially, with certain groups of metabolites not taken up until others 9 had been entirely depleted from the medium. Additionally, metabolite excretion 10 showed some complex patterns. Fitting non-linear equations (four-parameter 11 sigmoids) to individual metabolite data allowed us to model these changes for 12 13 metabolite uptake, and visualize them by back-projecting the curve-fit parameters 14 onto the original growth curves. These 'uptake window' plots clearly demonstrated 15 strain differences, with the uptake of some compounds being reversed in order 16 between different strains. Comparison of an undefined rich medium (LB) with a defined complex medium designed to mimic cystic fibrosis sputum showed many 17 differences, both qualitative and quantitative, with a greater proportion of excreted to 18 19 utilized metabolites in the defined medium. Extending the strain comparison to a 20 more closely related set of isolates showed it was possible to discriminate two 21 species of the Burkholderia cepacia complex based on uptake dynamics alone. We believe time-resolved metabolic footprinting could be a valuable tool for many 22 23 questions in bacteriology, including isolate comparisons, phenotyping deletion 24 mutants, and as a functional complement to taxonomic classifications.

1 INTRODUCTION

2

3 The increasing speed of gene discovery has exceeded our ability to understand gene 4 function, and one of the bottlenecks is the need for new, high throughput tools to 5 evaluate cellular phenotypes (22). Even in bacterial genomes less than 70% of genes 6 have an assigned putative function and fewer still are characterized biochemically. 7 Metabolic profiling approaches have shown great promise for providing these tools 8 for functional genomics and hypothesis generation (1, 6, 10, 18, 28, 43, 49), because 9 they offer complementary information to transcriptomics and proteomics, in particular 10 giving an integrated picture of information downstream of the genome (51). Various 11 aspects of cellular physiology like the levels of transcripts, proteins or protein activity 12 are altered in response to environmental cues or metabolite concentrations 13 themselves. In return, these changes are amplified in the metabolome to give an 14 accumulated – and highly sensitive – description of the physiological state of the 15 organism or cellular compartment (26, 45, 49). This extends to natural populations 16 that have multiple uncharacterized genetic changes such as an accumulation of 17 mutations, as well as sometimes-extensive genetic differences like pathogenicity 18 islands (21), which may interact to give complex phenotypes. Molecular phylogenetic 19 methods based on gene sequences have proved successful in classifying bacteria 20 into taxonomic groupings, but these may not always correspond to easily identifiable 21 pheno- or ecotypes (29, 33, 48). Hence additional methods for strain assessment 22 that could be related to function would still be valuable.

23

Metabolomics gives an integrated measurement of cellular phenotype, and is highly suited to quantitative analysis and description. In a microbial context, metabolomics

1 offers the additional advantage that there is only a single cell type, and little 2 compartmentation (at least in comparison to the equivalent problem in a multicellular organism). However, sampling intracellular metabolites without either changing their 3 4 relative concentrations or introducing contamination from supernatant metabolites is not straightforward, and research methods are still under active development by 5 6 different groups (7, 12, 15, 59, 62). In contrast, exometabolome or supernatant profiling ('metabolic footprinting') is simple, and extracellular metabolites can exhibit 7 8 very large changes in pool size (1, 27, 40, 45). These multiple advantages mean that 9 exometabolome analysis has already been employed for a number of diverse 10 applications, such as phenotyping of both single-gene deletion mutants as well as isolates from natural populations, although so far mostly for fungi rather than bacteria 11 12 (1, 2, 9, 25, 40, 48).

13

14 Because metabolism integrates information from gene expression and a wealth of 15 environmental cues, each organism will exhibit a distinct response, i.e. metabolic 16 pattern that takes into account all these factors. It is therefore unsurprising that these 17 patterns change with growth phase (1, 30). Despite this fact, it is currently common 18 practice to sample only at one or two time-points, mostly the end of growth, in 19 stationary phase (e.g. 48) and/or in mid-exponential phase (41, 52). In contrast, there 20 is ample evidence that cellular biochemistry changes during growth (1, 3, 8, 39). 21 Vertebrate studies have shown that explicitly considering 'through time' responses 22 (metabolic trajectories) adds considerably to the description and understanding of biological events (16, 23, 58). We therefore argue that new approaches that are 23 capable of integrating metabolic phenotypes over a range of conditions could be 24 25 extremely beneficial for microbiology.

2 In this study we have developed such an approach and evaluated it by monitoring 3 metabolic changes over the course of time in growing batch cultures. Time Resolved 4 Metabolic Footprinting (TReF) was used to compare the well-studied organisms 5 Escherichia coli and Pseudomonas aeruginosa. We demonstrate that TReF is 6 considerably more data-rich and informative than sampling at single time points and 7 show the usefulness of the approach in hypothesis generation and as a phenotyping 8 tool. We also show that TReF distinguishes isolates from the closely related 9 Burkholderia cepacia complex (Bcc) at the species level for B. cepacia and B. 10 cenocepacia, which is not the case for single timepoint analysis. The approach is 11 very general and would therefore benefit the broader application of metabolomics to 12 bacterial systems.

13

1 MATERIALS AND METHODS

2 Bacterial strains. We used the following strains in this study: Escherichia coli MG1655; the Pseudomonas aeruginosa wild type strains PA01 and PA14 (50), P. 3 aeruginosa PA0381 leu-38 str-2, a leucine auxotroph derived from PA01 (17); 4 B. cenocepacia LMG 16654, B. cenocepacia LMG 16659, B. cenocepacia LMG 5 18830, B. cenocepacia LMG 16656 (J2315), B. cenocepacia LMG 18863, B. cepacia 6 7 LMG, B. cepacia LMG 6963, B. cepacia LMG 6988, and B. cepacia LMG 18821. 8 Starter cultures for four biological replicates were set up by inoculating single 9 colonies into 5 ml of LB medium (10 g/L tryptone, 5 g yeast extract, 5 g NaCl) and growing overnight at 37°C, shaking at 150 rpm. The growth of PA01 was compared 10 11 under the same conditions in synthetic cystic fibrosis medium (SCFM), a complex defined medium designed to model nutrient status in sputum (46). These cultures 12 were used to inoculate 20 ml of LB or SCFM in 250 ml conical flasks and then grown 13 for 24 h at 37°C shaking at 150 rpm. 14

15

16 **Sampling:** 1 ml was taken from the culture at 0, 2, 4, 5, 6, 7, 8, 9, 10, 11, 12, and 24 17 hours for *E. coli*, *P. aeruginosa* PA01 and all *Burkholderia* strains. The *P. aeruginosa* PA14 and *P. aeruginosa* PA0381 cultures were sampled at 0, 2, 3, 4, 5, 6, 8, 10, 12, 18 14, 16, and 24 hours. (It should be noted that the total volumes sampled from each 19 20 culture would potentially change the cell physiology in comparison to an unsampled 21 flask; however, we were not aiming to model an unsampled culture.) For each 22 sample, 0.1 ml was mixed with 0.9 ml culture medium for determination of cell 23 density (OD₆₀₀). The remainder of the sample was centrifuged (16000 x g, RT) and 24 0.75 ml of the supernatant mixed with 0.2 ml NMR buffer (25 mM sodium azide, 0.25 M phosphate buffer pH 7, and 5 mM sodium 3-trimethylsilyl-2,2,3,3-²H₄-propionate 25

1 (TSP), in ${}^{2}\text{H}_{2}\text{O}$). The ${}^{2}\text{H}_{2}\text{O}$ provided a field frequency lock for the spectrometer and 2 the TSP served as an internal chemical shift reference.

3

4 ¹H NMR measurement: spectra were acquired on a Bruker Avance DRX600 NMR 5 spectrometer (Bruker BioSpin, Rheinstetten, Germany), with a magnetic field strength of 14.1 T and resulting ¹H resonance frequency of 600 MHz, equipped with 6 a 5 mm inverse flow probe. Samples were introduced using a Gilson flow-injection 7 8 autosampler. Spectra were acquired following the approach given in (4). Briefly, a 9 one-dimensional NOESY pulse sequence was used for water suppression; data were 10 acquired into 32 K data points over a spectral width of 12 kHz, with 8 dummy scans and 64 scans per sample, and an additional longitudinal relaxation recovery delay of 11 12 3.5 s per scan, giving a total recycle time of 5 s.

13

14 Spectral processing and data analysis: Spectra were processed in iNMR 2.5 15 (Nucleomatica, Molfetta, Italy). Free induction decays were multiplied by an 16 exponential apodization function equivalent to 0.5 Hz line broadening, followed by Fourier transformation. Spectra were manually phased and automated first order 17 baseline correction was applied. Spectral data between -0.5 and 10 ppm were then 18 19 imported into Matlab 2007b (MathWorks, Cambridge, UK) and normalized to the 20 integral of the TSP signal. Metabolites were assigned using in-house data, the 21 Chenomx NMR Suite 3.1 (Chenomx Inc., Edmonton, Canada) and the Biological Magnetic Resonance Databank metabolomics database (14). Signature peaks, i.e. 22 23 well-resolved resonances that could be easily assigned to one compound, were 24 identified from the spectra. Difference spectra were calculated in order to eliminate the influence of (non-biological) variation in media composition. For this, the 25

spectrum at time-point 0 h was subtracted from the spectra of other time-points of the same strain-replicate pair (i.e. all spectra sampled from the same flask). In addition to full resolution spectra, all analyses were carried out on spectra binned integrals representing the dominant resonances detected in fresh, non-inoculated medium. 153 integrals were fitted for LB, and 130 for SCFM. For the heatmap plots, the overall range of the resonance intensity changes was set to one and the changes were expressed relative to the starting values.

8

9 Modeling and pattern recognition analysis

10 We tested two different approaches to monitor the time-dependent changes in 11 metabolite concentration: (a) Linear regression analysis was carried out with both optical density at 600 nm (OD) and time as X variable. A cut-off value for goodness 12 of fit (R²=0.6) was determined by visual inspection of the fits. (b) Non-linear 13 14 regression of the data against time using a sigmoid curve model (Eq. 1) was carried 15 out using 'nlinfit' (Matlab statistics toolbox, Matlab). This resulted in fitting each 16 variable with four parameters, the amplitude of the curve, the 'half-life' (t_{50}) and the width of the decrease. Cut-offs for t_{50} (1-24 h), width (0-12 h) and relative error 17 18 (< 0.6) were imposed.

19
$$y = \frac{amplitude}{1 + e^{width}} + offset$$
[1]

20

The width is defined as the time that elapses for the exponent of e to go from 1 to -1. Growth rate differences (*E. coli* grows faster than the *Pseudomonas* strains) manifest themselves in higher t_{50} values for slower growing than faster growing strains, and these quantitative growth rate effects complicate the elucidation of qualitative

differences that are particularly interesting for strain comparison purposes. Therefore, the sigmoid parameters were corrected for growth-curve bias before pattern recognition: the OD values were also fitted to the same non-linear model (Eq. 1). The amplitude was divided by the amplitude of the OD, and the t_{50} was expressed relative to the t_{50} of the growth curve by subtracting the t_{50} of each individual growth curve and dividing the resulting values by the width of the growth curve (Eq. 2).

 $\Delta t_{50_i} = \frac{t_{50_i} - t_{50_{OD}}}{width_{OD}}$

[2]

7

8

-

9

10

The fitting parameters were then mean-centered and used as inputs for hierarchical 11 principal components analysis (H-PCA, (61)). As a first step for H-PCA, PCA was 12 13 carried out on the corrected amplitude, the corrected 'half-life' and the width. To 14 account for the missing values introduced by employing cut-off values, the Non-linear 15 Iterative Partial Least Squares (NIPALS)-PCA algorithm was used. The three resulting scores blocks were normalized by division by their highest values to give 16 17 each 'scores block' equal importance and used as input variables for a second-level PCA. 18

- 1 RESULTS
- 2

Time Resolved Metabolic Footprinting (TReF) provides additional biological information compared to single time-point analysis

5 Initially, we monitored changes in Luria broth culture supernatant during the growth of 6 the widely studied Gram-negative bacteria Escherichia coli (wild type MG1655) and 7 Pseudomonas aeruginosa (wild types PA01, PA14 and the leucine auxotroph 8 PA0381, which was derived from PA01 (17)). Additionally, growth of PA01 in a 9 defined medium (SCFM) (46) was compared. The ¹H NMR spectra showed a complex mixture of small molecules, the majority of which could be readily assigned 10 11 by comparison of their multiplicity and chemical shift to published or online values (Table 1). There were also a smaller number of resonances, which we have not yet 12 13 assigned (0.91d, 1.07d, 1.19m, 1.27m, 1.36d, 2.69m, 3.81s, 5.85d, 5.88d, 6.03d, 14 6.08d, 6.15d, 6.30d, 6.86m).

15

16 Over the course of growth there were major changes in the metabolite composition of the growth media. This is illustrated in Fig. 1A, which shows the chemical shift region 17 from 2 to 4 ppm of one LB grown culture of *P. aeruginosa* PA01 over time. At 18 19 compound level, TReF revealed differences in the rates of uptake of individual 20 compounds, as shown for three amino acids in a *P. aeruginosa* PA01 LB cultures. Alanine was taken up first from the medium, followed by threonine and then leucine 21 22 (Fig. 1B). This clear time separation shows different modes of compound utilization 23 during growth, and this differential compound utilization was observed for multiple 24 compounds and in all investigated isolates. Further, the order in which compounds 25 were utilized varied, but was reproducible at isolate level. These differences would

have been missed by single time-point profiling at 12 or 24 h and clearly indicate that
comparative metabolomics would benefit from the application of TReF-based
approaches, as differences can be highly growth-phase dependent.

4

Figure 2 provides a summary of the changes that were observed in the investigated 5 cultures over time. Fig. 2A-E is a heatmap representation of averaged difference 6 7 spectra depicting both uptake and secretion at compound level, clearly showing 8 patterns of metabolite secretion and uptake that differed greatly between the different 9 strains and media. Four different modes were identified. a) Constant depletion: the 10 majority of metabolites in the medium decreased constantly over time (e.g. Fig. 1, Fig. 3B). b) Transient excretion, followed by depletion: some compounds (e.g. 11 acetate, Fig. 2F) were excreted during one growth phase and taken up during 12 13 another. c) Transient depletion, followed by excretion: all Pseudomonas strains first 14 took up formate, only to excrete it at later time-points (Fig. 2H). d) Constant 15 excretion: some compounds increased in a sigmoid fashion, e.g. an as-yet 16 unassigned doublet resonance at δ 1.10 ppm (probable methyl group signal from an organic acid, Fig. 2G). As shown in Fig. 2, the growth medium itself has a large 17 18 influence on the metabolite utilization and depletion patterns, with major differences 19 between *P. aeruginosa* PA01 grown in LB and in SCFM. The uptake behavior at the 20 compound level is summarized in Fig. 2 and Table 2. Based on these first observations, the differences in compound utilization and excretion were further 21 investigated and are discussed below. 22

23

Non-linear regression modeling can be used to describe metabolite utilization
 over time

Most of the NMR-detectable resonances decreased over the course of growth (Fig 1 2 2I,J). In order to further describe the changes in exometabolome composition over time, the concentration changes of individual metabolites were modeled by 3 regression. Linear regression against time was a poor descriptor of metabolite 4 consumption. Most of the NMR resonance intensities did not describe a straight line 5 when plotted against time and thus each modeled variable usually contained an 6 7 unacceptable amount of fitting error (as an example, the dotted line in Fig. 3B shows 8 the linear fit of the pyroglutamate resonance at 2.40 ppm in one *P. aeruginosa* PA01 culture). Only about one-third of the fitted resonances had an R² value greater than 9 10 0.6. For many compounds, the change in the resonance intensities roughly mirrored a growth curve and thus more closely resembled a straight line when plotted against 11 12 OD (data not shown). The fits were indeed slightly improved when cell density 13 (OD₆₀₀) rather than time was used as the X variable: about half the fitted resonances had R² values bigger than 0.6. However, the average correlation across all 14 15 resonances was still poor for both time and OD (R=0.48 for time, 0.56 for OD). 16 Instead, fits were significantly improved by using an appropriate non-linear model. A bacterial growth curve typically describes a sigmoid shape over time. Though the 17 intensities of most NMR resonances did not exactly mirror this growth curve, they did 18 19 decrease in a sigmoid fashion. Consequently, fitting sigmoid curves to the evolution 20 of the resonances over time markedly decreased errors for 'real' peaks as opposed to noise (solid line in Fig. 3B). Even after imposing stringent cut-off values for fit (see 21 22 methods), the dataset still contained about two-thirds of the resonances. Non-linear 23 fitting is well suited to study media depletion, but was less useful for secreted metabolites. 24

25

1 For the data successfully fitted by non-linear modeling, the time course of each 2 metabolite resonance was described by four parameters (Fig. 3A). Three parameters summarize the uptake characteristics for each metabolite: the relative decrease of 3 4 the resonance with time (amplitude); the time of uptake (t50); and the duration of uptake (width). The fourth parameter, the offset, i.e. the intensity at the start of the 5 6 experiment, does not represent meaningful information in this case, as we used 7 difference spectra for the analysis. Hence, the offset was zero (for the original data) 8 or close to zero (fitted data).

9

10 Uptake window plots visualize compound utilization

The parameters of the sigmoid equation can be used to obtain physiological 11 12 information for individual compounds. Both the t_{50} and the width are in units of time 13 with the t₅₀ defining the time point at which the amplitude has reached its half-way 14 point, i.e. when half of the compound has been utilized. The width is defined as the 15 time that elapses for the exponent of e to go from 1 to -1 (see methods) and roughly 16 translates to the duration in which the compound is taken up at the maximum rate, and thus defines a time span or "uptake window" for any fitted compound / resonance 17 lying around the compound t_{50} value (Figure 3). These 'uptake windows' can be 18 19 projected onto the OD₆₀₀ growth curves of the individual strains to visualize 20 differential compound uptake. Figures 4A-D show the projections of the uptake windows of seven compounds (alanine, leucine, threonine, asparagine, valine, 21 22 succinate, and the disaccharide trehalose) onto the growth curves of the E. coli and the three *P. aeruginosa* strains for LB. Each circle represents the t₅₀ value of one 23 24 compound for one biological replicate with the bars on either side representing the 25 width of the same compound.

2 These uptake window plots illustrate how TReF is able to elucidate similarities in and difference of compound utilization of strains, summarized with a single plot. Not only 3 4 did the uptake windows differ dramatically for the individual metabolites, but there was very clear separation between them - i.e. the different amino acids fell into 5 different 'utilization groups', which were separated along the growth curve. For 6 7 example, *P. aeruginosa* PA01 (grown in LB) did not take up threonine until after the 8 simultaneous depletion of alanine and asparagine. Leucine was then taken up after 9 threonine had been removed. This order was also observed for the two other 10 P. aeruginosa strains but was different in E. coli, with trehalose taken up before 11 alanine, and leucine not taken up at all.

12

1

13 Additionally, the plots provide evidence for significant differences between the three 14 P. aeruginosa strains. PA14 does not take up succinate in a sigmoidal fashion, 15 however the compound was quickly removed from the medium in all strains. 16 Interestingly, PA0381, originally derived from PA01, was shown to have lost its ability to utilize trehalose. This loss of function could be a side effect of the leucine 17 auxotrophy causing a metabolic network rearrangement. However, a more 18 19 parsimonious explanation is that the non-specific mutagenesis used to obtain the 20 leucine auxotroph phenotype (53) also affected one of the genes necessary for trehalose breakdown (the transporter or the trehalase). 21

22

23 Transient changes in the exometabolome and metabolite excretion

Apart from metabolite uptake, a large proportion of the detected resonances transiently increased or decreased during growth in both LB and SCFM (Fig. 2). As a

1 positive confirmation, we detected acetate production by *E. coli*, a known example of 2 overflow metabolism. Acetate is a fermentation product that accumulates at high growth rates, probably due to a rate bottleneck in aerobic metabolism (38); it was by 3 4 far the clearest example of overflow metabolism in our current study. When grown in LB, all *Pseudomonas* strains transiently excreted the amino acids valine and 5 tyrosine. In PA01 cultures, a singlet resonance at 2.24 ppm (putatively assigned as 6 7 acetaldehyde) showed similar excretion dynamics to those of valine. Interestingly, 8 this was not observed for the other *Pseudomonas* strains. In contrast, formate (Fig 9 2H) was taken up from the medium during the first couple of hours of growth, but was 10 excreted in stationary phase. In addition to these transient changes, a number of resonances increased proportionally to cell number over the course of growth, 11 including 6-hydroxynicotinate (all *Pseudomonas* strains), indole (*E. coli*), and uracil 12 13 (all strains).

14

15 Compound utilization and excretion are dramatically influenced by the 16 constituents of the growth media

It could be argued that the complexity of the responses we observed were partly 17 down to our using a complex and undefined growth medium. To that end, we 18 19 compared the exometabolome of *P. aeruginosa* PA01 grown in LB to that grown in 20 SCFM, a defined medium designed and shown to mimic conditions and utilization dynamics in cystic fibrosis sputum (46). Even though the cell density (as OD_{600}) in 21 22 different media did not differ greatly (data not shown), the choice of growth medium 23 had a dramatic effect on the dynamics of the exometabolome, affecting both 24 compound uptake and excretion (Figures 2 and 4E,F). Concerning compound 25 utilization, a comparison of the uptake windows for selected amino acids in the two

1 media (Table 2 and Figure 4E,F) revealed several trends. Some amino acids, such 2 as lysine, phenylalanine and leucine, were taken up later from LB than SCFM, which might hint at some sort of catabolite repression-like regulation in LB (see discussion). 3 4 In contrast, the uptake dynamics of alanine, glutamate or aspartate and arginine were relatively unaffected as they were taken up at an early stage in both cultures. In 5 6 terms of compound secretion, many more resonances increased when PA01 was 7 grown in SCFM compared to LB. The transient increases in tyrosine and valine were 8 also not observed in SCFM, but other resonances (1.07 d, 2.51 and 2.53 s) were 9 observed to increase transiently. Finally, the pattern of formate change (transient 10 decrease, followed by increase) was even more pronounced in SCFM.

11

12 **Potential application of TReF as a functional genomics tool**

13 Pattern recognition algorithms like PCA are widely used for multivariate data to 14 visualize and summarize metabolic differences by dimension reduction. It was 15 possible to separate E. coli and all P. aeruginosa strains using PCA on stationary 16 phase samples and the approach very clearly showed the metabolites responsible for the strain differences (Fig. 5). However, the plots also show how single time-point 17 profiling would miss the 'big picture', i.e. the metabolite concentration changes that 18 19 occur at other time-points. If, for example, the cultures were sampled at 12 h, valine 20 would appear to be excreted only by PA01 (Fig. 5E). In fact, PA14 and PA0381 also excrete valine at earlier time-points. Had the exometabolome been sampled at 24 h 21 22 only, valine would appear to be utilized by all three *P. aeruginosa* strains to roughly 23 the same extent. Additionally, the strains' leucine (Fig. 5F) utilization would look 24 roughly equivalent after 12 h, whereas, in fact, leucine uptake was slower and had a slightly greater amplitude in PA01 cultures. Of the discriminatory metabolites at 12 h, 25

1 only trehalose (Fig. 5D) would show the same qualitative difference between the 2 strain at all time-points. One advantage of the non-linear metabolite fitting is that the fit parameters summarize key biological endpoints (e.g. compound uptake rates) in a 3 4 compact way. Thus, by using the fit parameters as input for the multivariate analyses, it is possible to compare data in a principled way from different strains, which might 5 have slightly different growth rates, lag phase, etc. Naturally, each parameter could 6 7 be analyzed separately, but it is also possible to combine these in a single 8 hierarchical model (Fig. 5C).

9

10 As a test case for the resolution the TReF/H-PCA approach could offer, we analyzed 11 culture supernatants of two species (nine strains in total) of the closely related 12 Burkholderia cepacia complex. Single time-point profiling like that shown for 13 stationary phase (t=24h) samples only provided some possible species separation, 14 but with considerable overlap between the species groups (Fig. 6A, similar results for 15 other time-points, data not shown). An added complication for this data set was that 16 the strains showed large variations in growth rate, which were picked up by standard multivariate methods. However, the non-linear H-PCA approach showed a separation 17 of *B. cepacia* and *B. cenocepacia* along PC1 (Fig. 6B). Thus, while 'standard' 18 19 footprinting based on single time-points may be adequate for showing large 20 metabolic differences, it failed to fully represent the subtle metabolic differences 21 between the Bcc strains, which required the non-linear fit data. (We also tested H-22 PCA alone, i.e. a hierarchical model based on PCA for individual time-points without 23 any curve fitting, but this offered no advantages in comparison to analyzing single 24 time-points, and failed to separate the Bcc species; data not shown).

25

2 DISCUSSION

We have developed a time resolved metabolic footprinting approach for bacteria that should be widely applicable. Considering changes in the culture medium over the whole course of growth provides information that would be lost in a single time point analysis.

7

8 Bacteria show 'multiauxic' uptake behavior on complex media

TReF revealed differential compound uptake for all investigated strains, and for both 9 10 a rich and a defined medium (LB and SCFM). The existence of a complex regulatory 11 network leading to highly adaptable uptake dynamics is not surprising. In rich (or 12 defined multi-compound) media, expression and translation of the transporter systems and catabolic pathways need to be controlled. The genomes of the 13 Pseudomonas species group contain over 300 known or putative nutrient uptake 14 15 systems (56). Expressing all inducible transporters and catabolic pathways at once 16 will not be energetically favorable, and so a form of multiauxic growth and sequential compound uptake, like that observed here, is the likely outcome - although the 17 18 extent of the differentiation between compound utilization classes during apparently 19 exponential growth was surprising. A number of previous studies, albeit mostly not 20 using rich media, have hinted at the complexity of the regulation at hand (e.g. 3, 19, 21 30).

22

Catabolite repression is a generic mechanism for regulation of substrate usage, and, for example, succinate represses arginine catabolism in *Pseudomonas aeruginosa* (42). ArgR controls the aerobic catabolism of arginine in *P. aeruginosa* (47), and also controls the levels of OprD, a porin for basic amino acids (44) and a serine

1 transporter (32). It is therefore logical that our data show that succinate depletion precedes the utilization of not only arginine, but also a number of other amino acids 2 (Fig. 4). As a second example, lysine was depleted at an earlier growth phase in 3 4 SCFM than in LB. Lysine can be imported by the specific permease LysP (54), but also by the putative basic amino acid ABC transporter PA5152-PA5155 (24). 5 Transposon mutants within this operon were severely impaired in growth on ornithine 6 as a single carbon source (24), so this transporter clearly contributes to P. 7 8 aeruginosa's ability to use ornithine. Hence it is highly probable that the high 9 concentrations of ornithine in SCFM would induce expression of PA5152-PA5155, 10 thereby potentially simultaneously increasing the potential rate of lysine uptake. These examples show how an untargetted approach can generate eminently testable 11 12 hypotheses.

13

14 The influence of media composition on uptake and excretion

15 In addition to utilization, we studied compound excretion. Various compounds like 16 acetate, valine and tyrosine were excreted transiently, whereas others like 6-hydroxy nicotinic acid or indole constantly increased over the course of growth for P. 17 aeruginosa and E. coli, respectively. Formate had a particularly surprising utilization 18 19 profile, with depletion followed by subsequent excretion; the precise reason is not 20 clear at this moment. Compound excretion is a well-known phenomenon for 21 biotechnologically interesting compounds in bacteria like Corynebacterium 22 glutamicum (11, 40). A number of fundamental principles that lead to compound excretion have been formulated (11). The obvious explanation for a compound 23 entering the culture medium is excretion of a product that bacteria "want" to excrete. 24 This is the case for signaling molecules like quorum sensing (QS) signals. Our data 25

1 show excretion of indole in E. coli, which was suggested to have extracellular signaling properties (60). It should be noted that *P. aeruginosa* in particular is known 2 for producing a suite of QS metabolites, which might be expected to be visible in the 3 4 medium; the reason that we do not identify more QS-related changes is probably just that NMR has relatively high detection limits. However the TReF principle would be 5 6 identical if using a more sensitive analytical platform, such as many techniques based on mass spectrometry. Additionally, compounds might also be excreted 7 8 because of overflow metabolism, limited catabolism, and deregulated anabolism (11). This "relief-valve"-function has previously been suggested for the aromatic amino 9 10 acid exporter (ArAE, formerly AaeAB) in *E. coli* (57). This transporter has recently been functionally annotated in *P. aeruginosa* (24), so tyrosine could be excreted by 11 12 P. aeruginosa when grown in LB to relieve intracellular stress. Valine might be 13 excreted due to similar reasons by a so-far unindentified transporter. Interestingly, 14 tyrosine and valine were only excreted into LB, not SCFM. Finally, the increase of 6-15 hydroxynicotinic acid in *P. aeruginosa* cultures is probably due to limited catabolism 16 of NAD or niacin, and has been used as a diagnostic marker of *P. aeruginosa* 17 infection (20).

18

19 Species discrimination in the *Burkholderia cepacia* complex

An important and general question is to what degree *phenotypic* metabolomic data is informative about *genotype*, i.e. strain relatedness, as opposed to, say, ecotype, which could be a convergent result of adaptation. Previous studies have used both endo- and exometabolome profiling to address this in yeast and bacteria (33, 34, 48); it is clearly a complex question, as metabolomic data have shown both apparent

clustering by ecotype, with additional genetic within-cluster separation, and also high
 between-strain metabolic variability that mostly correlated with genotype divisions.

3

4 The *P. aeruginosa* and *E. coli* profiles were dramatically different, with the order of uptake of specific metabolites reversed (Fig. 4). However this is perhaps not 5 6 surprising given these are very different organisms. We decided to carry out a more 7 realistic test: whether differences could still be observed for a set of much more 8 closely related bacteria. We chose two species of the Bcc (Burkholderia cepacia and 9 Burkholderia cenocepacia, represented here by 4 and 5 independent isolates 10 respectively) as a model comparison. The Bcc is a collection of genotypically distinct 11 but phenotypically similar species within the genus Burkholderia (13, 37). Some Bcc 12 members are opportunistic pathogens that can cause serious infections in patients 13 with chronic granulomatous disease (CGD) or cystic fibrosis (35, 37), while some are 14 found in the rhizosphere of important crops like maize and can protect these plants 15 from fungal infection (5). Species-level identification of Bcc members is difficult and 16 species are still frequently misidentified, especially using commercial identification 17 systems (31). Single-gene phylogenies showed that *B. cepacia* and *B. cenocepacia* 18 are especially similar genetically even within the Bcc (36, 55), meaning these two 19 species formed a stringent test for our approach. The non-linear fitting TReF 20 approach was nevertheless able to discriminate the isolates into species groups. It 21 cannot be concluded at this point that this could therefore be used as a general tool 22 for Bcc taxonomy (more isolates would need to be tested to derive robust 23 conclusions about metabolic differences in these species), but serves as a proof-ofprinciple that our approach of modelling the full time course of metabolic changes 24

1 can provide additional and biologically meaningful data over single timepoint

2 analyses.

3

4 Conclusion

5 have shown potential microbiological applications of time-dependent We 6 exometabolome profiling. Modeling of the amino acid utilization of E. coli and 7 P. aeruginosa demonstrated an unexpected complexity of regulation. In addition, the 8 same approach was shown to have clear advantages over single-time point profiling. 9 TReF allowed comparison of the physiology of bacteria in different nutritional 10 environments, and our data clearly demonstrates that marked differences could be 11 found. We believe time-dependent metabolic profiling could be a valuable addition to 12 the fields of bacterial physiology, functional genomics, and as a tool for strain 13 comparison, both as a complement to traditional taxonomies, and also for 14 investigating properties such as strain-specific virulence. It is still likely that single-15 time-point metabolic footprinting will be preferred for many studies, simply because it 16 requires analysis of fewer replicates. We see TReF having a complementary role, for in-depth phenotype analysis of a smaller number of strains - which might well, for 17 18 instance, have been initially selected through single-time-point profiling.

19

20

21 Acknowledgements

22 VB was funded by a divisional studentship.

1	
2	REFERENCES

3		
4 5	1.	Allen, J., H. M. Davey, D. Broadhurst, J. K. Heald, J. J. Rowland, S. G.
6		Oliver, and D. B. Kell. 2003. High-throughput classification of yeast mutants for
7		functional genomics using metabolic footprinting. Nat Biotechnol 21:692-696.
8	2.	Allen, J., H. M. Davey, D. Broadhurst, J. J. Rowland, S. G. Oliver, and D. B.
9		Kell. 2004. Discrimination of modes of action of antifungal substances by use of
10		metabolic footprinting. Appl Environ Microbiol 70:6157-6165.
11	3.	Baev, M. V., D. Baev, A. J. Radek, and J. W. Campbell. 2006. Growth of
12		Escherichia coli MG1655 on LB medium: determining metabolic strategy with
13		transcriptional microarrays. Appl Microbiol Biotechnol 71:323-328.
14	4.	Beckonert, O., H. C. Keun, T. M. Ebbels, J. Bundy, E. Holmes, J. C. Lindon,
15		and J. K. Nicholson. 2007. Metabolic profiling, metabolomic and metabonomic
16		procedures for NMR spectroscopy of urine, plasma, serum and tissue extracts.
17		Nat Protoc 2 :2692-2703.
18	5.	Bevivino, A., V. Peggion, L. Chiarini, S. Tabacchioni, C. Cantale, and C.
19		Dalmastri. 2005. Effect of Fusarium verticillioides on maize-root-associated
20		Burkholderia cenocepacia populations. Res Microbiol 156:974-983.
21	6.	Bino, R. J., R. D. Hall, O. Fiehn, J. Kopka, K. Saito, J. Draper, B. J. Nikolau,
22		P. Mendes, U. Roessner-Tunali, M. H. Beale, R. N. Trethewey, B. M. Lange,
23		E. S. Wurtele, and L. W. Sumner. 2004. Potential of metabolomics as a
24		functional genomics tool. Trends Plant Sci 9:418-425.

1	7.	Bolten, C. J., P. Kiefer, F. Letisse, J. C. Portais, and C. Wittmann. 2007.
2		Sampling for metabolome analysis of microorganisms. Anal Chem 79:3843-
3		3849.
4	8.	Buckstein, M. H., J. He, and H. Rubin. 2008. Characterization of nucleotide
5		pools as a function of physiological state in Escherichia coli. J Bacteriol
6		190 :718-726.
7	9.	Bundy, J. G., B. Papp, R. Harmston, R. A. Browne, E. M. Clayson, N.
8		Burton, R. J. Reece, S. G. Oliver, and K. M. Brindle. 2007. Evaluation of
9		predicted network modules in yeast metabolism using NMR-based metabolite
10		profiling. Genome Res 17:510-519.
11	10.	Bundy, J. G., T. L. Willey, R. S. Castell, D. J. Ellar, and K. M. Brindle. 2005.
12		Discrimination of pathogenic clinical isolates and laboratory strains of Bacillus
13		cereus by NMR-based metabolomic profiling. FEMS Microbiol Lett 242:127-136.
14	11.	Burkovski, A., and R. Kramer. 2002. Bacterial amino acid transport proteins:
15		occurrence, functions, and significance for biotechnological applications. Appl
16		Microbiol Biotechnol 58:265-274.
17	12.	Canelas, A., C. Ras, P. ten, Angela, D. van, Jan, J. Heijnen, and G. van,
18		Walter. 2008. Leakage-free rapid quenching technique for yeast metabolomics.
19		Metabolomics 4:226-239.
20	13.	Chiarini, L., A. Bevivino, C. Dalmastri, S. Tabacchioni, and P. Visca. 2006.
21		Burkholderia cepacia complex species: health hazards and biotechnological
22		potential. Trends Microbiol 14:277-286.
23	14.	Cui, Q., I. A. Lewis, A. D. Hegeman, M. E. Anderson, J. Li, C. F. Schulte, W.
24		M. Westler, H. R. Eghbalnia, M. R. Sussman, and J. L. Markley. 2008.

Metabolite identification via the Madison Metabolomics Consortium Database.
 Nat Biotechnol **26**:162-164.

3	15.	de Koning, W., and K. van Dam. 1992. A method for the determination of
4		changes of glycolytic metabolites in yeast on a subsecond time scale using
5		extraction at neutral pH. Anal Biochem 204:118-123.
6	16.	Ebbels, T. M., H. C. Keun, O. P. Beckonert, M. E. Bollard, J. C. Lindon, E.
7		Holmes, and J. K. Nicholson. 2007. Prediction and classification of drug
8		toxicity using probabilistic modeling of temporal metabolic data: the consortium
9		on metabonomic toxicology screening approach. J Proteome Res 6:4407-4422.
10	17.	Fyfe, J. A., and J. R. Govan. 1980. Alginate synthesis in mucoid Pseudomonas
11		aeruginosa: a chromosomal locus involved in control. J Gen Microbiol 119:443-
12		450.
13	18.	Goodacre, R., S. Vaidyanathan, W. B. Dunn, G. G. Harrigan, and D. B. Kell.
14		2004. Metabolomics by numbers: acquiring and understanding global metabolite
15		data. Trends Biotechnol 22:245-252.
16	19.	Gschaedler, A., N. Thi Le, and J. Boudrant. 1994. Glucose and acetate
17		influences on the behavior of the recombinant strain Escherichia coli HB 101
18		(GAPDH). J Ind Microbiol 13:225-232.
19	20.	Gupta, A., M. Dwivedi, G. A. Nagana Gowda, A. Ayyagari, A. A. Mahdi, M.
20		Bhandari, and C. L. Khetrapal. 2005. ¹ H NMR spectroscopy in the diagnosis of
21		Pseudomonas aeruginosa-induced urinary tract infection. NMR Biomed 18:293-
22		299.
23	21.	Hacker, J., and J. B. Kaper. 2000. Pathogenicity islands and the evolution of

24 microbes. Annu Rev Microbiol **54**:641-679.

Hocquette, J. F. 2005. Where are we in genomics? J Physiol Pharmacol 56
 Suppl 3:37-70.

3	23.	Holmes, E., F. W. Bonner, B. C. Sweatman, J. C. Lindon, C. R. Beddell, E.
4		Rahr, and J. K. Nicholson. 1992. Nuclear magnetic resonance spectroscopy
5		and pattern recognition analysis of the biochemical processes associated with
6		the progression of and recovery from nephrotoxic lesions in the rat induced by
7		mercury(II) chloride and 2-bromoethanamine. Mol Pharmacol 42:922-930.
8	24.	Johnson, D. A., S. G. Tetu, K. Phillippy, J. Chen, Q. Ren, and I. T. Paulsen.
9		2008. High-throughput phenotypic characterization of Pseudomonas aeruginosa
10		membrane transport genes. PLoS Genet 4 :e1000211.
11	25.	Kaderbhai, N. N., D. I. Broadhurst, D. I. Ellis, R. Goodacre, and D. B. Kell.
12		2003. Functional genomics via metabolic footprinting: monitoring metabolite
13		secretion by Escherichia coli tryptophan metabolism mutants using FT-IR and
14		direct injection electrospray mass spectrometry. Comp. Funct. Genom. 4:376-
15		391.
16	26.	Kell, D. B. 2006. Systems biology, metabolic modelling and metabolomics in
17		drug discovery and development. Drug Discov Today 11 :1085-1092.
18	27.	Kell, D. B., M. Brown, H. M. Davey, W. B. Dunn, I. Spasic, and S. G. Oliver.
19		2005. Metabolic footprinting and systems biology: the medium is the message.
20		Nat Rev Microbiol 3:557-565.
21	28.	Kell, D. B., and S. G. Oliver. 2004. Here is the evidence, now what is the
22		hypothesis? The complementary roles of inductive and hypothesis-driven
23		science in the post-genomic era. Bioessays 26 :99-105.

1	29.	Konstantinidis, K. T., A. Ramette, and J. M. Tiedje. 2006. The bacterial
2		species definition in the genomic era. Philos Trans R Soc Lond B Biol Sci
3		361 :1929-1940.
4	30.	Lee, R., A. S. Ptolemy, L. Niewczas, and P. Britz-McKibbin. 2007. Integrative
5		metabolomics for characterizing unknown low-abundance metabolites by
6		capillary electrophoresis-mass spectrometry with computer simulations. Anal
7		Chem 79 :403-415.
8	31.	LiPuma, J. J. 2007. Update on Burkholderia nomenclature and resistance. Clin.
9		Microbiol. Newsletter 29 :65-69.
10	32.	Lu, C. D., Z. Yang, and W. Li. 2004. Transcriptome analysis of the ArgR
11		regulon in Pseudomonas aeruginosa. J Bacteriol 186:3855-3861.
12	33.	Mackenzie, D. A., M. Defernez, W. B. Dunn, M. Brown, L. J. Fuller, S. R. de
13		Herrera, A. Gunther, S. A. James, J. Eagles, M. Philo, R. Goodacre, and I.
14		N. Roberts. 2008. Relatedness of medically important strains of
15		Saccharomyces cerevisiae as revealed by phylogenetics and metabolomics.
16		Yeast 25 :501-512.
17	34.	Maharjan, R. P., and T. Ferenci. 2005. Metabolomic diversity in the species
18		Escherichia coli and its relationship to genetic population structure.
19		Metabolomics 1:235-242.
20	35.	Mahenthiralingam, E., A. Baldwin, and C. G. Dowson. 2008. Burkholderia
21		cepacia complex bacteria: opportunistic pathogens with important natural
22		biology. J Appl Microbiol 104:1539-1551.
23	36.	Mahenthiralingam, E., J. Bischof, S. K. Byrne, C. Radomski, J. E. Davies, Y.
24		Av-Gay, and P. Vandamme. 2000. DNA-Based diagnostic approaches for
25		identification of Burkholderia cepacia complex, Burkholderia vietnamiensis,

1		Burkholderia multivorans, Burkholderia stabilis, and Burkholderia cepacia
2		genomovars I and III. J Clin Microbiol 38 :3165-3173.
3	37.	Mahenthiralingam, E., T. A. Urban, and J. B. Goldberg. 2005. The
4		multifarious, multireplicon Burkholderia cepacia complex. Nat Rev Microbiol
5		3 :144-156.
6	38.	Majewski, R. A., and M. M. Domach. 1990. Simple constrained-optimization
7		view of acetate overflow in <i>E. coli</i> . Biotechnol Bioeng 35 :732-738.
8	39.	Majors, P. D., J. S. McLean, and J. C. Scholten. 2008. NMR bioreactor
9		development for live in-situ microbial functional analysis. J Magn Reson
10		192 :159-166.
11	40.	Mapelli, V., L. Olsson, and J. Nielsen. 2008. Metabolic footprinting in
12		microbiology: methods and applications in functional genomics and
13		biotechnology. Trends Biotechnol 26:490-497.
14	41.	Mas, S., S. G. Villas-Boas, M. E. Hansen, M. Akesson, and J. Nielsen. 2007.
15		A comparison of direct infusion MS and GC-MS for metabolic footprinting of
16		yeast mutants. Biotechnol Bioeng 96:1014-1022.
17	42.	Mercenier, A., J. P. Simon, D. Haas, and V. Stalon. 1980. Catabolism of L-
18		arginine by Pseudomonas aeruginosa. J Gen Microbiol 116 :381-389.
19	43.	Nicholson, J. K., J. Connelly, J. C. Lindon, and E. Holmes. 2002.
20		Metabonomics: a platform for studying drug toxicity and gene function. Nat Rev
21		Drug Discov 1 :153-161.
22	44.	Ochs, M. M., C. D. Lu, R. E. Hancock, and A. T. Abdelal. 1999. Amino acid-
23		mediated induction of the basic amino acid-specific outer membrane porin OprD
24		from Pseudomonas aeruginosa. J Bacteriol 181 :5426-5432.

1	45.	Oliver, S. G., M. K. Winson, D. B. Kell, and F. Baganz. 1998. Systematic
2		functional analysis of the yeast genome. Trends Biotechnol 16 :373-378.
3	46.	Palmer, K. L., L. M. Aye, and M. Whiteley. 2007. Nutritional cues control
4		Pseudomonas aeruginosa multicellular behavior in cystic fibrosis sputum. J
5		Bacteriol 189 :8079-8087.
6	47.	Park, S. M., C. D. Lu, and A. T. Abdelal. 1997. Cloning and characterization of
7		argR, a gene that participates in regulation of arginine biosynthesis and
8		catabolism in <i>Pseudomonas aeruginosa</i> PAO1. J Bacteriol 179 :5300-5308.
9	48.	Pope, G. A., D. A. MacKenzie, M. Defernez, M. A. Aroso, L. J. Fuller, F. A.
10		Mellon, W. B. Dunn, M. Brown, R. Goodacre, D. B. Kell, M. E. Marvin, E. J.
11		Louis, and I. N. Roberts. 2007. Metabolic footprinting as a tool for
12		discriminating between brewing yeasts. Yeast 24:667-679.
13	49.	Raamsdonk, L. M., B. Teusink, D. Broadhurst, N. S. Zhang, A. Hayes, M. C.
14		Walsh, J. A. Berden, K. M. Brindle, D. B. Kell, J. J. Rowland, H. V.
15		Westerhoff, D. van, K, and S. G. Oliver. 2001. A functional genomics strategy
16		that uses metabolome data to reveal the phenotype of silent mutations. Nat
17		Biotechnol 19 :45-50.
18	50.	Rahme, L. G., M. W. Tan, L. Le, S. M. Wong, R. G. Tompkins, S. B.
19		Calderwood, and F. M. Ausubel. 1997. Use of model plant hosts to identify
20		Pseudomonas aeruginosa virulence factors. Proc Natl Acad Sci U S A
21		94 :13245-13250.
22	51.	Ryan, D., and K. Robards. 2006. Metabolomics: The greatest omics of them
23		all? Anal Chem 78 :7954-7958.
24	52.	Sariyar-Akbulut, B., A. Salman-Dilgimen, S. Ceylan, S. Perk, A. A. Denizci,
25		and D. Kazan. 2008. Preliminary phenotypic characterization of newly isolated

1		halophilic microorganisms by footprinting: a rapid metabolome analysis. Arch
2		Microbiol 189 :19-26.
3	53.	Stanisich, V., and B. W. Holloway. 1969. Conjugation in Pseudomonas
4		aeruginosa. Genetics 61:327-339.
5	54.	Steffes, C., J. Ellis, J. Wu, and B. P. Rosen. 1992. The IysP gene encodes the
6		lysine-specific permease. J Bacteriol 174 :3242-3249.
7	55.	Tabacchioni, S., L. Ferri, G. Manno, M. Mentasti, P. Cocchi, S. Campana, N.
8		Ravenni, G. Taccetti, C. Dalmastri, L. Chiarini, A. Bevivino, and R. Fani.
9		2008. Use of the gyrB gene to discriminate among species of the Burkholderia
10		cepacia complex. FEMS Microbiol Lett 281:175-182.
11	56.	Tamber, S., and R. E. Hancock. 2003. On the mechanism of solute uptake in
12		Pseudomonas. Front Biosci 8:s472-83.
13	57.	Van Dyk, T. K., L. J. Templeton, K. A. Cantera, P. L. Sharpe, and F. S.
14		Sariaslani. 2004. Characterization of the Escherichia coli AaeAB efflux pump: a
15		metabolic relief valve? J Bacteriol 186 :7196-7204.
16	58.	Viant, M. R., J. G. Bundy, C. A. Pincetich, J. S. de Ropp, and R. S.
17		Tjeerdema. 2005. NMR-derived developmental metabolic trajectories: an
18		approach for visualizing the toxic actions of trichloroethylene during
19		embryogenesis. Metabolomics 1:149-158.
20	59.	Villas-Boas, S. G., and P. Bruheim. 2007. Cold glycerol-saline: the promising
21		quenching solution for accurate intracellular metabolite analysis of microbial
22		cells. Anal Biochem 370 :87-97.
23	60.	Wang, D., X. Ding, and P. N. Rather. 2001. Indole can act as an extracellular
24		signal in Escherichia coli. J Bacteriol 183:4210-4216.

1	61.	Westerhuis, J. A., T. Kourti, and J. F. MacGregor. 1998. Analysis of
2		multiblock and hierarchical PCA and PLS models. Journal of Chemometrics
3		12 :301-321.
4	62.	Winder, C. L., W. B. Dunn, S. Schuler, D. Broadhurst, R. Jarvis, G. M.
5		Stephens, and R. Goodacre. 2008. Global metabolic profiling of Escherichia
6		coli cultures: an evaluation of methods for quenching and extraction of
7		intracellular metabolites. Anal Chem 80:2939-2948.
8		
9		

1 TABLES AND FIGURE LEGENDS

2 3

Table 1. List of assigned NMR-visible resonances in LB (note that the metabolites
listed here may have other resonances: table includes only the most
characteristic and well-resolved resonances). Resonances in bold font were
used for non-linear fitting of compounds.

Compound	Compound Assigned resonance frequency (ppm)						
Acetate ^a	1.92						
Acetaldehyde ^a	2.24						
Adenosine ^a	6.08	8.26	8.34				
Alanine ^a	1.48	3.79					
Arginine ^a	1.69	1.73	1.75	1.91	3.25	3.78	
Asparagine ^b	1.72	2.86	2.96	4.00			
Aspartate ^a	2.68	2.82	3.91				
Formate ^a	8.46						
Glucose ^a	3.39	5.24					
Glutamate ^a	2.07	2.35	3.74				
Glycine ^a	3.57						
Glycine-betaine ^a	3.27	3.90					
Histidine (not							
fitted) ^a	3.11	3.14	3.31	7.07	7.88		
6-							
hydroxynicotinate ^b	6.62	8.07					
Indole ^d	6.61	7.18	7.27	7.42	7.56	7.72	
Isoleucine ^a	0.94	1.01	1.25	1.26	3.68	3.74	
Lactate ^c	1.33	4.12	. = -				
Leucine ^a	0.96	0.97	1.72	3.74			
Lysine ^a	1.46	1.48	1.73	1.89	1.91	3.03	
Methionine ^a	2.12	2.14	2.65				
Methionine-S-	0.74	0.70	0.00				
oxide ^b	2.74	2.76	2.93				
Nicotinic acid ^a	8.61	8.94					
Pyrimidine							
nucleotide ^a	5.91						
Ornithine ^c	3.81						
Phenylalanine ^a	3.11	3.28	4.01	7.33	7.39	7.43	
Pyroglutamate ^b	2.06	2.39	2.42	2.51	7.98	-	
Serine ^a	3.79	3.85	3.96				
Succinate ^b	2.41	_	-				
Threonine ^a	1.33	3.59	4.26				

Trehalose ^a	3.46	3.65	3.83	3.86	3.88	5.20
Tryptophan ^b	3.31	7.29	7.55	7.74		
Tyrosine ^a	3.07	3.22	3.31	3.94	6.90	7.20
Uracil ^a	5.82	7.55				
Valine ^a	0.99	1.05	2.28	3.62		
Unassigned						
metabolite						
(potential						
quinolone).	7.68	8.10				

- 1 a: observed in both LB and SCFM.
- 2 b: observed in LB only.
- 3 c: observed in SCFM only.
- 4 d: observed for *E. coli* only (not tested in SCFM).

- Table 2. Comparison of fitted metabolite t_{50} values (h) for *P. aeruginosa* PA01 grown
- in LB and SCFM.

	LB	SCFM	Difference ^a
Tyrosine	14.8	6.5	-8.3
Valine	15.8	8.5	-7.3
Phenylalanine	8.8	5.0	-3.8
Lysine	11.3	8.0	-3.3
Leucine	9.6	7.0	-2.5
Isoleucine	8.1	7.0	-1.2
Aspartate	3.1	2.2	-0.9
Arginine	4.0	3.5	-0.5
Glycine	5.3	5.0	-0.3
Glutamate	2.9	2.8	-0.2
Alanine	3.5	3.4	-0.1
Serine	2.7	4.3	1.6
Threonine	5.8	7.7	2.0
		not	
Asparagine	2.3	observed	-
Methionine	not utilized not	11.8	-
Ornithine	observed	4.0 not	-
Tryptophan	4.7	observed	-

Tryptophan4.7observed-a: 'Difference' refers to difference between t50 in SCFM compared to LB medium, i.e.

the lower the value, the earlier metabolite was taken up in SCFM compared to LB.

6 7

- Figure 1. A: section of 600 MHz ¹H NMR spectra (4—2 ppm) for a single *P*. *aeruginosa* PA01 culture over a growth curve. Time-specific metabolic changes are
 clearly seen. B: single compound utilization data for three selected metabolites for *P*. *aeruginosa* PA01. Error bars = SEM (n = 4).
- 6
- 7

Figure 2: Metabolite changes in different media and different strains across the ocurse of growth. Heatmaps (panels A - E): each row represents a metabolite, or a peak from an as-yet unassigned metabolite. Blue represents decrease in concentration, and red represents increase in concentration. Note that panels B - Ecan be directly compared visually, but the metabolites in panel A do not line up directly with B - E. Row for metabolite '6HN / indole' represents 6-hydroxynicotinate for *P. aeruginosa* strains, and indole for *E. coli*.

15 A: *P. aeruginosa* PA01, synthetic cystic fibrosis medium.

- 16 B: *P. aeruginosa* PA01, LB.
- 17 C: *P. aeruginosa* PA14, LB.
- 18 D: *P. aeruginosa* PA0381, LB.

19 E: *E. coli*, LB.

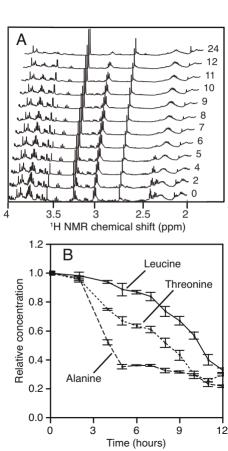
20 Selected metabolites with different modes of utilization/production are then shown in 21 detail in the bottom half of the figure (error bars represent ± SEM):

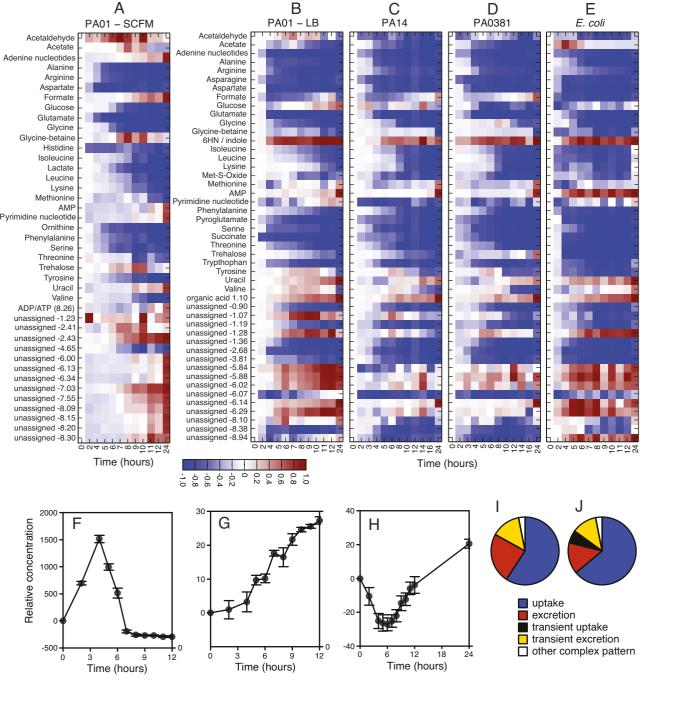
- 22 F: acetate, *E. coli*. Transient increase in metabolite concentration.
- G: unassigned metabolite, *E. coli*, peak at δ 1.10 ppm. Steady increase in
 metabolite concentration.
- H: formate, *P. aeruginosa* PA01, LB. Transient decrease in metabolite
 concentration followed by subsequent production.

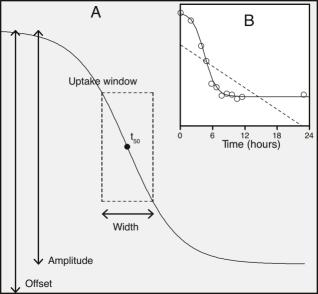
1	An overall comparison of the different modes is then shown as pie charts
2	(percentage of assigned metabolites that change in some way during growth).
3	I: <i>P. aeruginosa</i> PA01, SCFM.
4	J: <i>P. aeruginosa</i> PA01, LB.
5	
6	
7	
8	Figure 3. A: Schematic showing the parameters for non-linear curve fitting. B (inset):
9	curve fit for a representative compound (pyroglutamate) for P. aeruginosa
10	PA01. Solid line indicates sigmoid fit; dotted line indicates much poorer linear
11	fit.
12	
13	
14	Figure 4. Uptake window plots for seven example compounds for all four bacterial
15	strains. Compound t_{50} is back-projected upon the actual culture growth curve,
16	i.e. all biological replicates are shown. The 'error bars' represent calculated
17	width (see Fig. 2 for illustration of t_{50} and width). Note that both abscissa (time)
18	and ordinate (OD_{600}) have been scaled such that growth curve maxima are set
19	at 100%, to facilitate comparison across different strains. A: E. coli. B: P.
20	aeruginosa PA01. C: P. aeruginosa PA14. D: P. aeruginosa PA0381. The
21	remaining two panels compare uptake windows for P. aeruginosa PA01 for
22	two different media, LB and synthetic cystic fibrosis medium (SCFM). Note
23	that glucose is plotted (not trehalose as for panel A), as glucose is higher
24	concentration in SCFM. E: F:

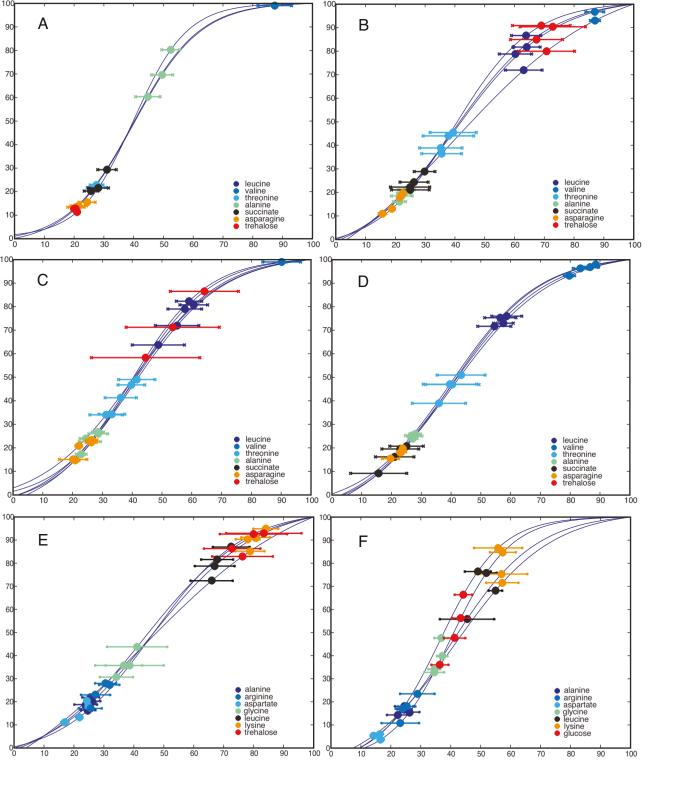
- 1
- 2 Figure 5. A: Principal components analysis for 12 h data, scores plot of axes 1 and 2. Filled circles: E. coli. Empty circles: P. aeruginosa PA01. Empty triangles: P. 3 4 aeruginosa PA14. Empty squares: P. aeruginosa PA0381. PCs 1 and 2 explained 87% and 8% of the variance in the data, respectively. 5 B: loadings plot for analysis shown in A. Variables corresponding to assigned 6 7 metabolite bins for leucine, valine, and trehalose are labelled directly on the 8 plot. C: Hierarchical principal components analysis of fitted time-course data. Figure 9 10 symbols are the same as for A. PCs 1 and 2 explained 50% and 33% of the 11 variance in the data, respectively. D: Trehalose utilization during growth for four strains. Solid black line: E. coli. 12 13 Solid grey line: *P. aeruginosa* PA01. Dashed line (long dashes): *P. aeruginosa* 14 PA14. Dashed line (short dashes): *P. aeruginosa* PA0381. 15 E: Valine utilization during growth for four strains. Line styles as for D. 16 F: Leucine utilization during growth for four strains. Line styles as for D. 17 18 19 Figure 6. Comparison of single-timepoint and nonlinear fitted metabolite data for four 20 Burkholderia cepacia (unfilled symbols) and five Burkholderia cenocepacia (filled symbols) isolates: principal components scores plots, axis 1 v axis 2. Different 21 22 symbol shapes represent different individual isolates. 23 A: Single-timepoint analysis does not discriminate all isolates into species. 24 PCs 1 and 2 explained 55% and 39% of the variance in the data, respectively.

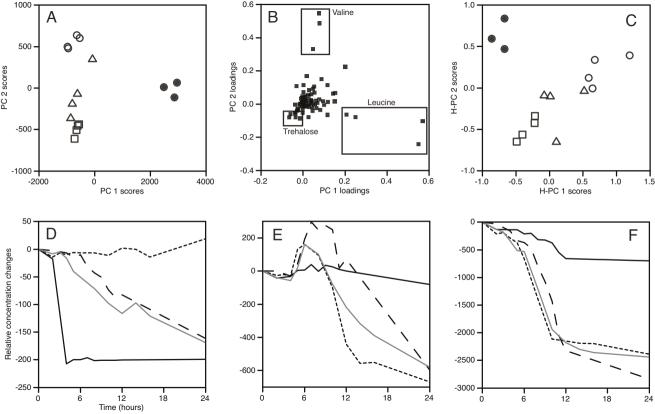
B: Fitted metabolite data (TReF) shows that species are discriminated along
 PC 1 across different isolates. PCs 1 and 2 explained 35% and 25% of the variance
 in the data, respectively.

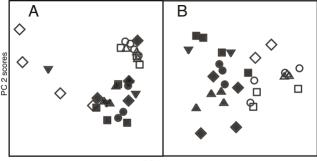












PC 1 scores